*Molecular Vision* 2017; 23:219-227 <http://www.molvis.org/molvis/v23/219>
Received 27 August 2016 | Accepted 10 April 2017 | Published 12 April 2017



# UVB promotes the initiation of uveitic inflammatory injury in vivo and is attenuated by UV-blocking protection

**Yi-Ching Shao,[1,2] Jyh-Cheng Liou,[1,2,3] Chan-Yen Kuo,[4] Yun-Shan Tsai,[2,5] En-Chieh Lin,[5,6] Ching-Ju Hsieh,[6,7] Si-Ping Lin,[2,5] Bo-Yie Chen[1,2,5]**

**(The first three authors contributed equally to this work.)**

*[1]Department of Ophthalmology, Chung Shan Medical University Hospital, Taichung, Taiwan; [2]Department of Optometry, Chung Shan Medical University, Taichung, Taiwan; [3]Institute of Medicine, Chung Shan Medical University, Taichung, Taiwan; [4]Institute of Systems Biology and Bioinformatics, National Central University, Jhongli, Taiwan; [5]Institute of Optometry, Chung Shan Medical University, Taichung, Taiwan; [6]Department of Ophthalmology, Taipei City Hospital, Taipei, Taiwan; [7]Department of Optometry, University of Kang Ning, Taipei, Taiwan*

**Purpose:** Uveitic inflammatory injury can cause irreversible visual loss; however, no single animal model recapitulates all the characteristics of human uveitis. Ultraviolet radiation (UVR) is one of the risk factors for uveitis, but the role of UVR in the pathogenesis of uveitic injury is unclear. The aim of this study was to elucidate whether UVB promotes the initiation of, and subsequently contributes to, uveitic inflammatory injury.

**Methods:** Mice were assigned to either a blank control group or one of three UVB treatment groups: no protection, protection with Nelfilcon A contact lens (Food and Drug Administration [FDA] class II, about 46.8% UVB transmittance), or protection with Etafilcon A contact lens (FDA class IV, about 0.55% UVB transmittance). The contact lenses acted as blocking barriers against UVR. After the application of UVR, pathologic injuries were determined with slit-lamp microscopy and histologic examination.

**Results:** Compared with the intact status of the controls, the anterior eyes of the UVB groups showed pathologic alterations in physiologic properties and tissue integrity. UVR promoted anterior uveitic inflammatory injury, with expansion of the hyperemic iris vessels, over-production of aqueous humor protein, disruption of the blood–aqueous barrier, and embedding of infiltrative leukocytes inside the iridocorneal angle. However, blockage of UVR in vivo retarded the progression of uveitic inflammatory injury. The highest level of UV protection in the Etafilcon A group resulted in greater inhibition of uveitic inflammatory injury than that in the Nelfilcon A group.

**Conclusions:** This study demonstrates that UVB initiated and promoted uveitic inflammatory injury. UV protection is needed for the clinical management of anterior uveitis. The Etafilcon A lenses provide better protection of the anterior segment of the eye against UVB damage compared with the Nelfilcon A lenses.

Ultraviolet radiation (UVR) can lead to various ocular abnormalities; UVB confers a higher risk of pathogenesis than UVA [1,2]. The pathology and extent of UVR damage are associated with its duration and energy intensity [3-5], and involve major ocular pathogenesis, including corneal distortion, photokeratitis [6-11], photoconjunctivitis [9], and cataractogenesis [12]. Photo-oxidation and inflammatory injury induced by UVR play a critical role in the complex process of pathological progression in the eye [7,9,11,13]. Therefore, there is great demand for effective strategies aimed at reducing UVR-associated visual problems. In particular, the beneficial effects of UV-blocking soft contact lenses [8,11,12] or UV-blocking spectacle lenses [10] on the cornea and visual performance have been investigated in vivo using animal models.

Uveitis is a sight-threatening disease and broadly classified into anterior, intermediate, and posterior based on eye anatomic involvement. Leukocyte recruitment in the anterior chamber or embedment inside the iridocorneal angle are the major pathologic characteristics of anterior uveitis [14-16]. The etiology is difficult to define in humans, but it can be induced by autoimmune interference, injury, infection, or toxins in animal. However, no single animal model recapitulates all characteristics of human uveitis. Furthermore, the potential of excessive UVR to initiate or promote uveitic injury remains to be elucidated.

UV protection strategies have been proposed in the prevention of uveitis and may dramatically reduce the morbidity and improve the quality of care in patients with uveitis. It has previously been observed that repeated UVB radiation in mouse eyes promotes the infiltration of

Correspondence to: Bo-Yie Chen, Department of Optometry, Institute of Optometry, Chung Shan Medical University, No. 110, Chien-Kuo North Road, Taichung 402, Taiwan; Phone: +886-4-2473-0022 ext. 12319; FAX: +886-4-2324-8131; email: boychen@csmu.edu.tw

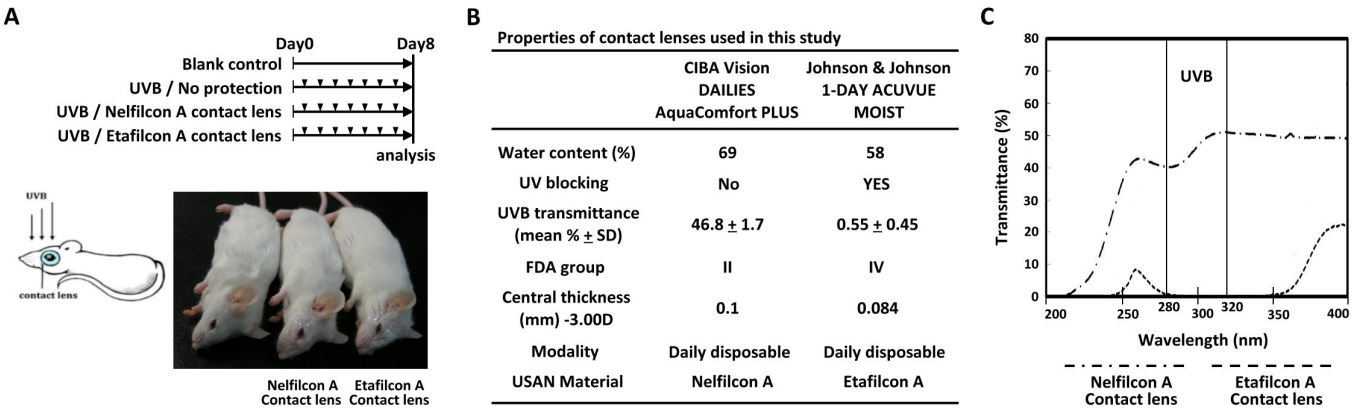


Figure 1. Experimental design. **A**: Daily ultraviolet B (UVB) light exposure (arrowhead) was performed for 7 days. No protection was given to the UVB group. The Etafilcon A and Nelfilcon A groups were provided protection by the contact lenses before exposure to ultraviolet radiation (UVR). **B**: The properties of the contact lenses used in this study. **C**: The UV transmittance properties of the Etafilcon A and Nelfilcon A contact lenses.

leukocytes into the anterior chamber that attack the corneal endothelium [7,10]. However, it is unclear whether this represents a failure of immune privilege or an overwhelming inflammatory response by UVR that exceeds the capacity of the eye. Therefore, the aim of this study was to elucidate whether UVB promotes the initiation of, and subsequently contributes to, uveitic inflammatory injury. To understand the role of UVR in the pathogenesis of uveitic inflammatory injury, we used the UVR barrier characteristics of contact lenses placed over the ocular surface of the mouse eyes before we administered UVR.

## METHODS

*Animals:* All animal procedures were approved by the Animal Care and Use Committee of Chung Shan Medical University and conformed to the guidelines that adhered to the ARVO Statement for use of animals in research. Female CD-1® Mouse, Nomenclature Crl: CD1 (ICR) mice (6–7-weeks-old) were purchased from BioLASCO Experimental Animal Center (Taiwan Co., Ltd, BioLASCO, Taipei, Taiwan). Only mice with normal eyes confirmed by slit lamp microscopy were included in the experiments.

*Experimental design:* A UVB lamp (peak wavelength at 312 nm: 280–320 nm; power density: 8 mW/cm$^2$; CN-6, Vilber Lourmat, France) was used, and the distance to the mouse cornea was approximately 15 cm (duration: 90 s, once daily for 7 days) [7,10]. Mice were assigned to either a blank control group (n = 12) or one of three UVB treatment groups (Figure 1 A): (1) without protection (UVB group; n = 12), (2) protection with Nelfilcon A contact lens (Nelfilcon A group; n = 12), and (3) protection with Etafilcon A contact lens (Etafilcon A group; n = 12). All contact lenses were used once per eye and discarded daily after UVR. Both eyes of each mouse were administered UVR (Figure 1A). After general anesthesia (Pentobarbital, 50 mg/kg, IP), the mouse eyes were covered individually with the relevant contact lenses and then exposed to UVB. Contact lens characteristics are shown in Figure 1B and the UV transmittance spectra in Figure 1C. The transmittance of UVB (280–320 nm) was approximately 46.8 ± 1.7% and 0.55 ± 0.45% in the Nelfilcon A and Etafilcon A contact lenses, respectively.

*Evaluation of the corneal surface and evaluation of uveitis:* The corneal surfaces of the left eyes of the anesthetized mice on day 8 were observed macroscopically and imaged. Analysis and scoring system details, including corneal smoothness and corneal lissamine green staining, have been previously described [9,10]. Anterior uveitic inflammatory injury sign and score were evaluated with slit-lamp microscopy on day 8 after UVR. The clinical severity of the uveitic inflammatory injury was graded by two independent observers according to the modification criteria described in Table 1.

*Histological analysis and protein analysis:* After euthanized by cervical dislocation on day 8, one of the mouse eyes was used for histological analysis and the other for protein analysis. Conventional tissue fixation, paraffin embedding, section preparation, hematoxylin-eosin, and immunostaining were performed as described in our previous studies [9,10]. Leukocyte infiltration was measured parallel to the eye's vertical meridian. Aqueous humor was collected with anterior chamber puncture with a 30-gauge needle on day 8. The protein concentration was determined using a protein quantification kit. The anterior segments of each eye (including the cornea, iris, and ciliary body) were isolated and homogenized individually in 50 µl lysis buffer (25 mM Tris-HCl, pH 7.5;

Table 1. Criteria of uveitis clinical scoring in mice.

| Clinical signs | Grade of Signs | Score |
|---|---|---|
| Iris hyperemia | Absent | 0 |
| | Mild | 1 |
| | Moderate | 2 |
| | Severe | 3 |
| Exudate in anterior chamber | Absent | 0 |
| | Present | 1 |
| Pupil | Normal | 0 |
| | Festooned | 1 |
| Limbal hyperemia | Absent | 0 |
| | Mild | 1 |
| | Moderate | 2 |
| | Severe | 3 |
| Maximum possible score | | 8 |

100 mM NaCl; and 1% v/v Nonidet P40) for western blotting analysis. The primary antibodies of anti-matrix metalloproteinases MMP9 (1/100 dilution for immunostaining; 1/100 dilution for western blotting; ab38898, Abcam, Cambridge, UK) were used in this study.

*Statistical analysis:* Data were obtained from individual mouse corneas. For all clinical examination evaluations, data were presented as mean ± standard deviation. Statistical analysis was performed using SPSS (SPSS, Inc., Chicago, IL), and graphs were generated using Microsoft Excel 2010. Data obtained from all groups were analyzed using the Kruskal–Wallis nonparametric ANOVA, and the Mann–Whitney U-test for pairwise comparisons in cases when the Kruskal–Wallis test was statistically significant. Incidence rates were analyzed using the independent-samples *t* test. Correlation between polymorphonuclear neutrophils (PMNs) counts in the corneal stroma, or the iridocorneal angle, and the transmittance strength of UVB was assessed with Pearson's correlation test. P values of less than 0.05 and 0.01 were considered statistically significant.

## RESULTS

*Contact lens UVR protection:* None of the control mice showed evidence of abnormalities on the corneal surface (Figure 2A,E). In contrast, the UVB group exhibited serious irregular distortion, shown as irregular white-light ring reflections (Figure 2B) and large dark blue devitalized epithelial staining (Figure 2F). The Nelfilcon A group corneas showed greater distortion (Figure 2C) and staining (Figure 2G) than those in the Etafilcon A group (Figure 2D,H, respectively); this result was statistically significantly different ($p<0.01$; Figure 2I,K). Contact lens protection reduced the incidence of corneal smoothness (score>2; Figure 2J) and corneal staining (score>2; Figure 2L) after UVR; the effect was statistically significantly greater in the Etafilcon A group compared with the Nelfilcon A group ($p<0.01$, Figure 2J; $p<0.05$, Figure 2L, respectively). These findings confirm UVR protective effects of contact lenses on the cornea in vivo.

*UVR role in the pathogenesis of uveitic injury in anterior eye segments:* Anterior uveitis inflammatory injury can be characterized by hyperemic change in the iris and the limbal vessel, and cellular exudates on the iris anterior surface. These symptoms were severe in the UVB group (Figure 2N), moderate in the Nelfilcon A group (Figure 2O), but absent in the Etafilcon A group (Figure 2P). The uveitis clinical scores were normal in the Etafilcon A group and statistically significantly lower than in the other two UVR groups ($p<0.01$; Figure 2Q). However, the scoring of the Nelfilcon A group was lower than that of the UVB group ($p<0.05$; Figure 2Q). After UVR, the aqueous humor protein concentration increased in the UVB group compared with that of the control (Figure 2R). This increase may be due to disruption of the blood–aqueous barrier. However, the reduction in the protein concentration occurred in the Nelfilcon A group after UVR, but this decrease was not statistically significant ($p = 0.08$; Figure 2R). However, the protein concentration was statistically significantly reduced in the Etafilcon A group ($p<0.01$; Figure 2R). This decrease confirmed that UVR participates in the pathogenesis of uveitic injury in the anterior segment of the eye.

*UVR contribution to the pathogenesis of cellular infiltrates in the iridocorneal angle of eyes:* Microscopically, the blank control group showed normal tissue integrity of the cornea (Figure 3A) and the iridocorneal angle (Figure 3E). The UVB group exhibited severe lesions, with a thin corneal epithelium, subepithelial bullae, and friable edematous stroma with infiltrating leukocytes (Figure 3B). Infiltrating leukocytes embedded inside the inferior iridocorneal angle were the predominant feature in the UVB group (Figure 3F). However, the Nelfilcon A group actually showed mild infiltrating leukocytes inside the iridocorneal angle (Figure 3G); in contrast, no evidence of abnormality was found in the Etafilcon A group (Figure 3H).

There were differences in the infiltrating leukocytes in the cornea (Figure 3I) and the iridocorneal angle (Figure 3K) between the study groups. Leukocyte infiltration was statistically significantly lower in the Nelfilcon A group compared with the UVB group ($p<0.01$); however, the infiltration was higher than in the Etafilcon A group (Figure 3I,K). This result may explained by the decrease in UVR transmittance due

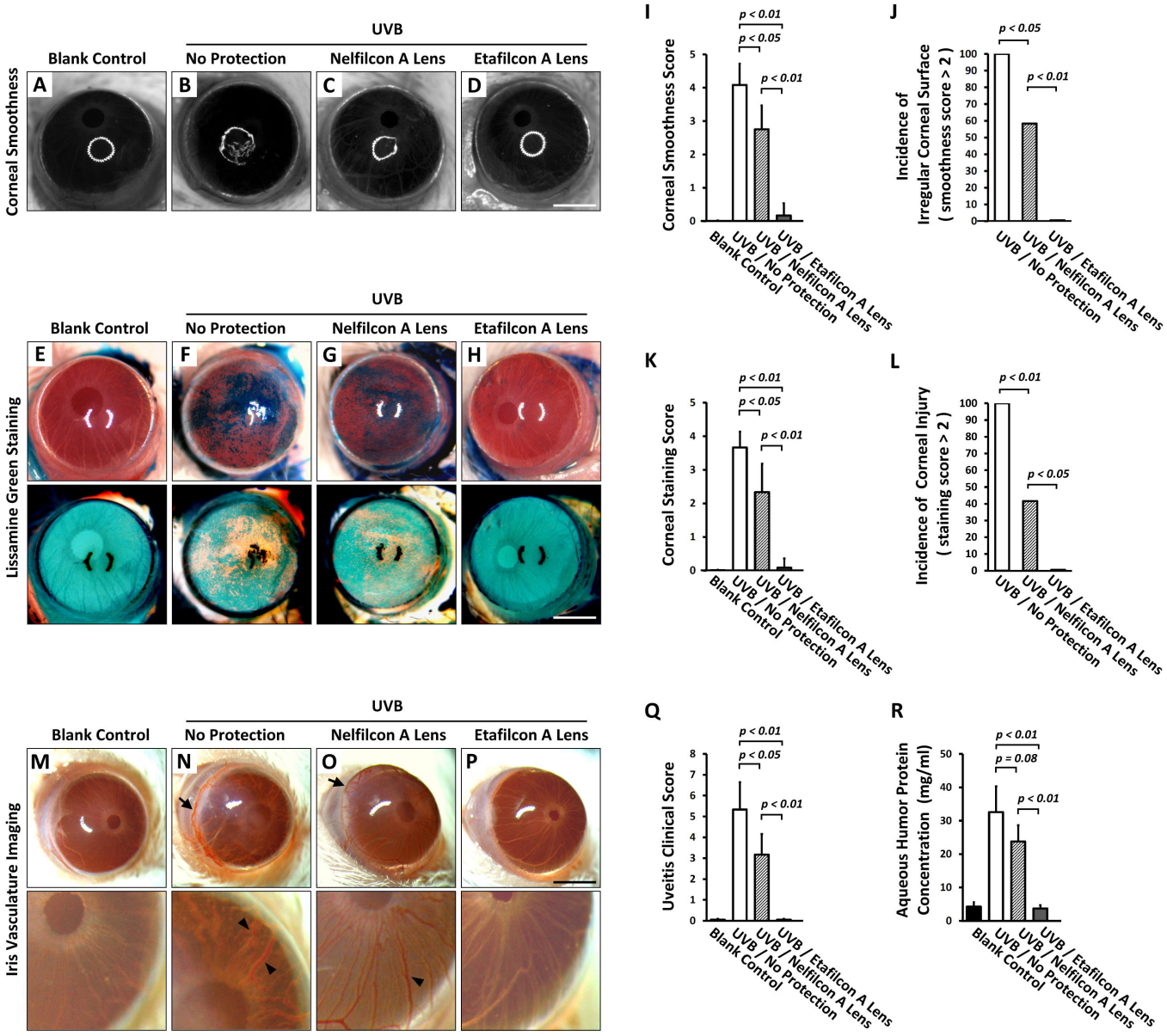


Figure 2. UVR role in the pathogenesis of corneal and uveitic injury in anterior eye segments. The clinical corneal evaluation of (**A-D**) corneal smoothness, and (**E-H**) lissamine green staining. **I**: Quantitative analysis of corneal smoothness (n = 12 per group). **J**: The incidence of corneal smoothness (score>2). **K**: Quantitative analysis of lissamine green staining (n = 12 per group). **L**: The incidence of corneal staining (score >2). **M-P**: The clinical evaluation of anterior iris surface. **N**,**O**: The hyperemic change in the vessel on the anterior iris surface (arrowhead) and limbus (arrow). **Q**: Quantitative analysis of the clinical uveitis score (n = 12 per group). **R**: Quantitative analysis of the aqueous humor protein concentration (n = 7 per group). All scale bars = 1.25 mm. p<0.05; p<0.01.

to Etafilcon A contact lens protection (Figure 1C). Leukocyte infiltration rates in the cornea (PMNs ≥15 cells/$\mu m^2$ × $10^5$) and the iridocorneal angle (PMNs ≥15 cells/section) are shown in Figure 3J,L; the rate was statistically significantly lower in the Nelfilcon A group compared with the UVB group (p<0.01). The efficacy of the inhibition of leukocyte infiltration was greater in the Etafilcon A group compared with the Nelfilcon A group (p<0.01 Figure 3J; p = 0.067, Figure 3L, respectively). This result suggests a correlation between leukocyte infiltration and UVB radiation intensity, or the efficacy of UV protection.

*UVR blocking can retard the initiation and progression of uveitic inflammatory injury:* Because reduced UVB transmittance strength improves the inhibitory efficacy of inflammatory injury in vivo, we analyzed the correlation between

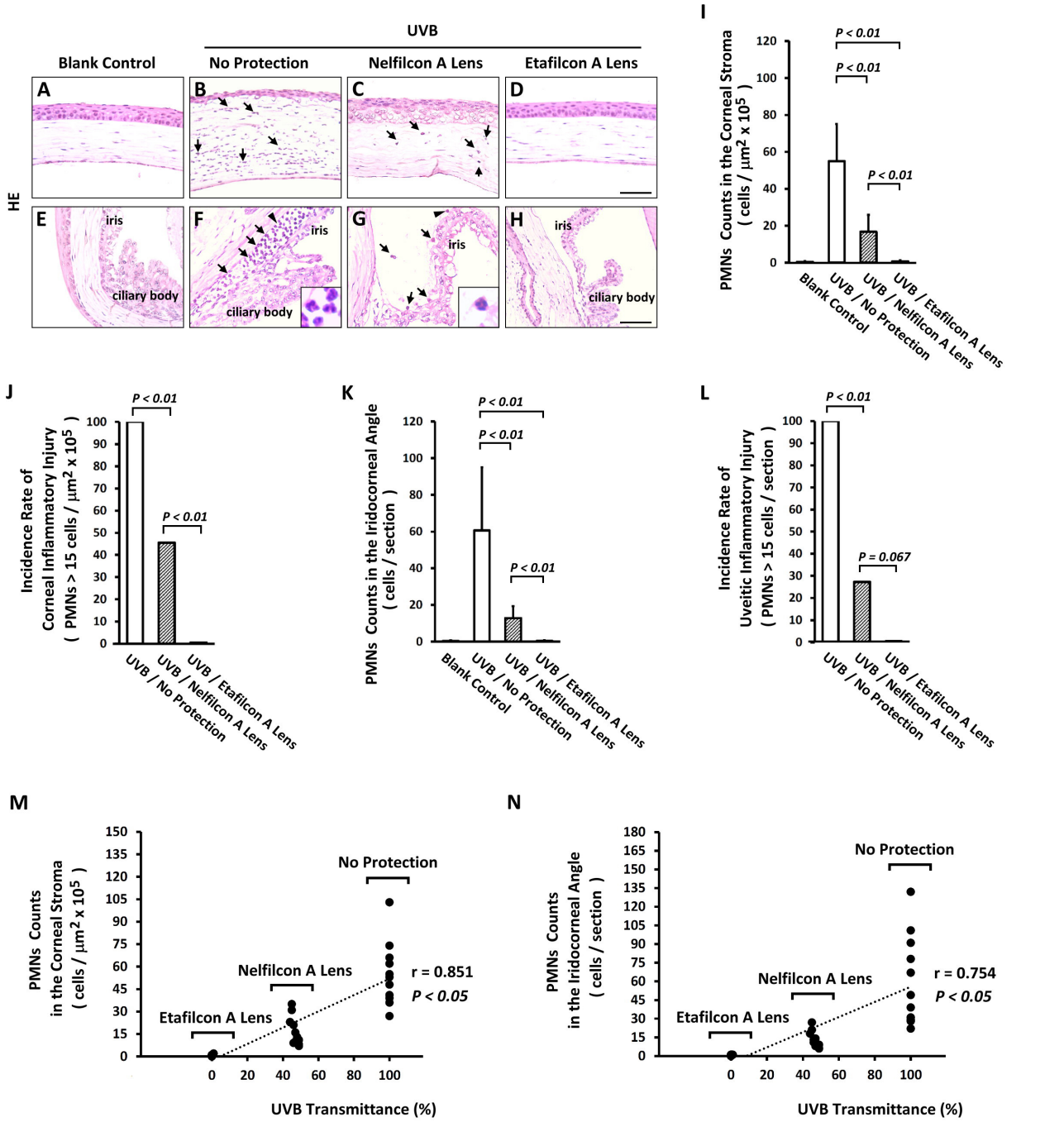


Figure 3. UVR contribution to the pathogenesis of cellular infiltrates in the iridocorneal angle of eyes. **A**-**H**: Histological analysis of anterior eye. **B**, **C**: The influx of PMNs in the corneal stroma (indicated by arrow), and (**F**, **G**) iridocorneal angle (indicated by arrow). **I**: Quantitative analysis of PMNs in the corneal stroma (n = 11 per group). **J**: The incidence of corneal inflammatory injury (n = 11 per group). **K**: Quantitative analysis of PMNs in the iridocorneal angle (n = 11 per group). **L**: The incidence of uveitic inflammatory injury (n = 11 per group). **M**, **N**: Scatterplots indicated a significant correlation between the reduction in UVR strength and PMN recruitment inhibition. Scale bars: 25 μm. The $p<0.05$ and $p<0.01$ indicated the statistically significant.

UVB transmittance strength and inflammatory pathogenesis. There was a statistically significant correlation between the reduction in UVR strength and inhibition of PMN recruitment in the corneal stroma (Pearson's correlation coefficient; $r = 0.851$, $p<0.05$; Figure 3M) and the iridocorneal angle (Pearson's correlation coefficient; $r = 0.754$, $p<0.05$; Figure 3N). This indicates that UVR blocking can retard the initiation and progression of uveitic inflammatory injury.

*The Etafilcon A lenses provide better protection of anterior segment of eye from UVB damage compared to the Nelfilcon A lenses:* To compare the efficacy of Etafilcon A lenses and Nelfilcon A lenses on UVR protection, an evaluation of both lenses, Etafilcon A (the right eye) and Nelfilcon A (the left eye), contralaterally was performed in the same mice to investigate the relative damage and protection after UVR. None of the Etafilcon A protection eyes (the right eye) showed evidence of abnormalities on the corneal surface (Figure 4A,B) or the iris anterior surface (Figure 4C) and microscopically showed normal tissue integrity of the cornea (Figure 4D) and the iridocorneal angle (Figure 4E). In contrast, the Nelfilcon A protection eyes (the left eye) showed irregular distortion of the cornea surface (Figure 4F), epithelial staining (Figure 4G), hyperemic iris (Figure 4H), and leukocyte influx in the corneal stroma (Figure 4I) and the iridocorneal angle (Figure 4J). Based on the results from the same animal, the evidence indicates that the Etafilcon A lenses provide better protection of the anterior segment of the eye from UVB damage compared with the Nelfilcon A lenses.

*Contribution of MMP9 protein produced by infiltrating leukocytes to uveitic inflammatory injury after UVR:* MMPs contribute to inflammatory injury. In this study, the MMP9 protein was predominately labeled and localized in infiltrating leukocytes (Figure 4L,N,P,R). Infiltrating leukocytes showed an abundance of MMP9 protein labeling in the iridocorneal angle of the eyes in the UVB group (Figure 4L,P) and the Nelfilcon A protecting eye group (left eye; Figure 4N,R). However, the MMP9 protein can contribute to the degradation of blood barrier structure molecules and leukocyte extravasation from blood vessels. Alternatively, the MMP9 protein may also destroy the blood–aqueous barrier resulting in an over-loading of inflammatory cells and exudate recruitment into the aqueous humor. In contrast, there was no evidence of the MMP9 protein in the control group (Figure 4K,O) and the Etafilcon A protecting eyes group (right eye; Figure 4M,Q). The expression of the MMP9 protein in the anterior segment tissues (including the cornea, iris, and ciliary body) was analyzed and confirmed with western blotting (Figure 4S). The level of the MMP9 protein statistically significantly increased in the corneas of the UVB group compared with those of the control group. In the same animal, the Etafilcon A protecting eye (right eye) showed more inhibition of the level of the MMP9 protein than that of the Nelfilcon A protecting eye (left eye) after UVR (Figure 4S,T).

## DISCUSSION

Elucidating the novel mechanisms that contribute to intraocular inflammatory diseases (collectively considered uveitis) and developing new insights is of great clinical importance. UVR-based animal models on corneal inflammatory injury have been proposed as useful approaches that consistently translate to human corneal pathology. In the present study, we demonstrated that UVB initiates the pathologic progression of uveitic inflammatory injury, involving infiltrating leukocyte embedment into the iridocorneal angle of the eye. However, limitations with this UVB trigger model of uveitic inflammatory injury exist in regard to comparability with human clinical characteristics.

UVB contributed to the initiation of inflammatory injury in the anterior eye, including the cornea, iris, ciliary body, and iridocorneal angle, which caused disruption of the blood–aqueous barrier resulting in over-loading of exudates into the aqueous humor. We used the UVR barrier properties of contact lenses, Etafilcon A and Nelfilcon A, which were placed on the ocular surface of mice eyes to retard the transmitted strength of UVR to confirm the triggering role of UVB in intraocular inflammatory injury. In the Etafilcon A group (the best UVB-blocking protection), there was no evidence of uveitic or corneal inflammatory injury after UVR. In contrast, the Nelfilcon A group showed a moderate clinical uveitis score, indicating that uveitic inflammatory injury occurred involving mild embedding of infiltrating leukocytes into the iridocorneal angle of the eye. Noticeably, the incidence rate of uveitic inflammatory injury, calculated by PMN counts in the iridocorneal angle (≥15 cells per section), statistically significantly decreased in the Etafilcon A group compared with the Nelfilcon A group (Figure 3L). However, the UVB group had a higher clinical uveitis score and infiltrating leukocyte rate than those of the contact lens protection groups. UV blocking by Etafilcon A contact lenses was shown to retard the source UVR and statistically significantly reduce inflammatory injury in the cornea and the iridocorneal angle. Additionally, the level of uveitic inflammatory injury indicated a statistically significant correlation with the strength of the transmitted UVB (Figure 3N). Additionally, the evidence indicates that the Etafilcon A lenses provide better protection of the anterior segment of the eye from UVB damage and from its relative

inflammation injury compared to the Nelfilcon A lens in a same animal (Figure 4). Therefore, these results indicate that UVR, especially UVB, applied through the cornea can directly destroy the blood–aqueous barrier and contribute to uveitic inflammatory injury in the anterior eye.

The major pathogenic mechanisms of anterior uveitis are unclear; clinically, they are usually classified as infectious or non-infectious [15]. Endotoxin-induced uveitis (EIU) is an infectious experimental model that mimics intraocular inflammation in humans, involving blood–aqueous barrier disruption, cellular infiltration, and protein extravasation into the anterior chambers [17-19]. PMNs are the most abundant type of infiltrating cell types surrounding the iris-ciliary body complexes in EIU [17,18]. It is well-known that transcription factor NF-κB, MMPs, and proinflammatory factors play a critical role in the pathogenesis of uveitic inflammatory injury in EIU [20-22]. UVB radiation has been indicated to induce the upregulation of NF-κB and MMPs in the mouse cornea [7-9]. The expression and localization of the MMP9 protein with infiltrating PMNs in the anterior chamber

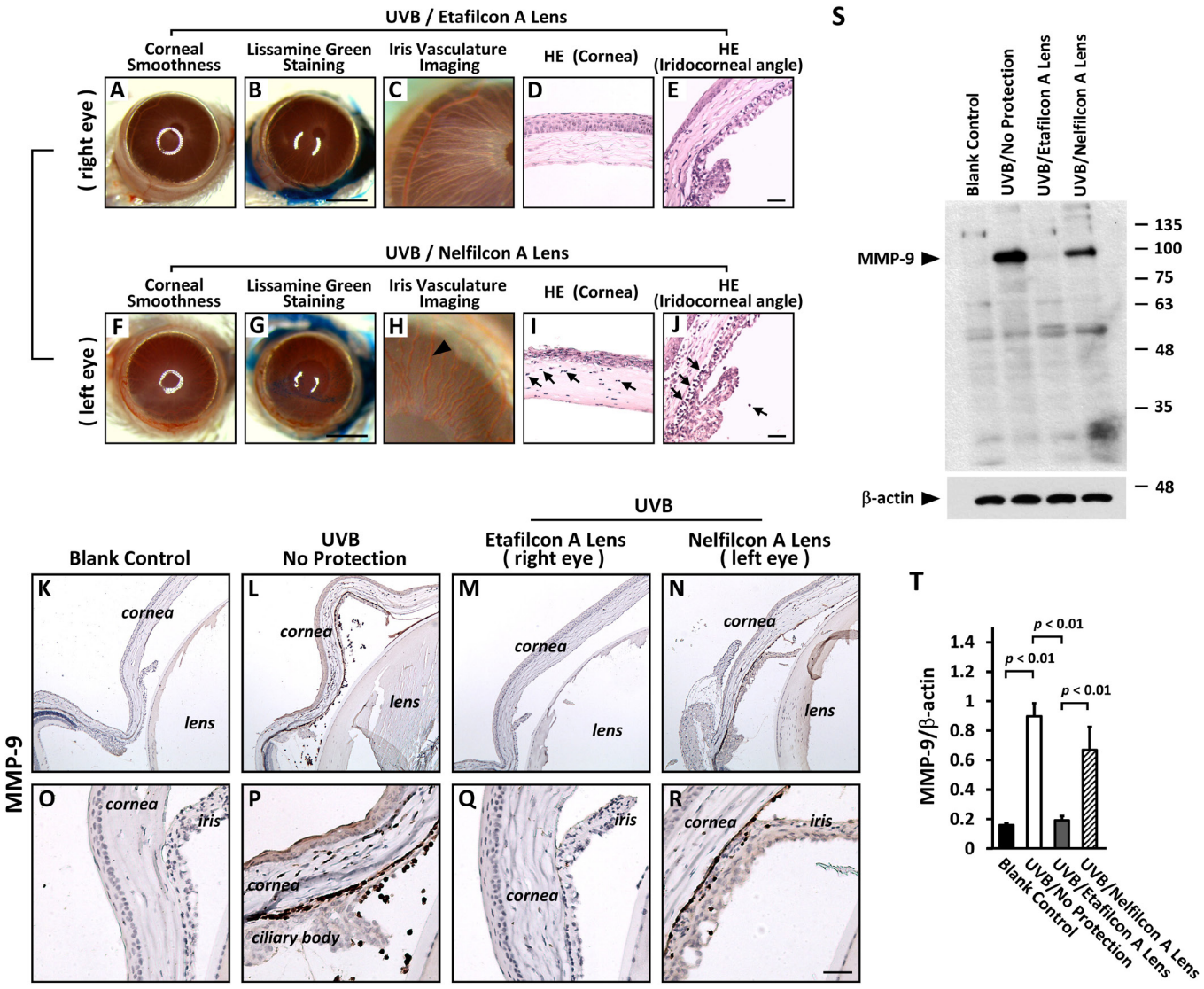


Figure 4. Contribution of MMP-9 protein produced by infiltrating leukocytes to uveitic inflammatory injury after UVR. Both lenses, Etafilcon A (right eye; **A**-**E**) and Nelfilcon A (left eye; **F**-**J**) contralaterally performed evaluation in a same mice to investigate the relative damage and protection after UVR. The arrowhead in **H** indicate the hyperemic iris. The arrow in **I** and **J** indicate the infiltrating leukocytes. **K**-**R**: The expression of MMP-9 protein was found in the infiltrating leukocytes of corneal stroma (**P**), anterior chamber (**L**, **N**), and iridocorneal angle (**P**, **R**) after UVR. **S**: The protein levels of MMP-9 was evaluated by western blotting. **T**: Quantitative analysis of MMP-9 protein in the anterior segment of eye (n=4 per group). Scale bars: 25 µm. The p<0.01 indicated the statistically significant.

after UVR were recorded in the present study, particularly in the UVB group (without protection). Additionally, excess production of MMPs might be a critical mechanism by which recruiting PMNs gain access to aqueous humor from the uvea [23,24]. However, matrix remodeling of the blood–aqueous barrier, was attributed to these proteolytically active enzymes. Nonetheless, the subsequent inflammatory response and proinflammatory cytokine interference in the blood–aqueous barrier and the inflammatory injury in this UVR model are still not fully understood. However, there may be differences in the mechanisms of uveitic inflammatory injury between UVR and EIU animal models.

Previous reports have indicated that the amount of UVB rays from sunlight could reach approximately 0.18 J/cm$^2$ per hour to the human eye surface in the Northeastern United States [25]. In the present animal study, the daily UVB dose was used at 0.72 J/cm$^2$, equivalent or close to 4 h of daily sunlight exposure in the real lives of many people. However, the biologic effects of UVB might differ in the mouse eye and the human eye. Additionally, the risk factors for the total energy or the light intensity of UVB regarding the initiation of the process of corneal or uveitis inflammatory injury might also be different.

This study presents a unique platform for determining the role of UVR in the pathogenesis of anterior uveitic injury. By performing histopathological analysis, multiple intraocular inflammatory injuries could be obtained from the same sample, providing a powerful means to dissect the interplay between UVR and uveitic disease pathogenesis. We describe the use of a UV-blocking approach for the amelioration of UVR-mediated cellular infiltration in the iridocorneal angle of mice eyes. However, although the UV-blocking contact lenses used are powerful experimental tools, we do not recommend direct use of them in the clinical management of uveitis. Nonetheless, application of our study approach for understanding the pathogenesis of non-infectious anterior uveitis can counteract limitations of the EIU model [17-19] or the classical autoimmune model [19-24,26], and its utility can be expanded into other fields such as ocular pharmacology. Future studies should expand research involving the biomarker analysis to further reveal the important cellular infiltration dynamics involved in the resolution of UVR triggered intraocular inflammatory injury, with the potential to be therapeutically manipulated.

## ACKNOWLEDGMENTS

This work was supported by a grant (CSH-2013-A-037) to Yi-Ching Shao from the Chung Shan Medical University Hospital, Taichung, Taiwan; and partly by a grant (MOST 103–2320-B-040–012-MY2) to BY Chen from the Ministry of Science and Technology, Taiwan. A substantial part of this work was performed in the Instrument Center of Chung Shan Medical University and supported by both the Ministry of Education and Chung Shan Medical University. The authors thank David Pei-Cheng Lin and Han-Hsin Chang for their assistance with different aspects of the study.

## REFERENCES

1. Taylor HR. The biological effects of UV-B on the eye. Photochem Photobiol 1989; 50:489-92. [PMID: 2687903].
2. DePry J, Brescoll J, Szczotka-Flynn L, Rambhatla P, Lim HW, Cooper K. Phototherapy-related ophthalmologic disorders. Clin Dermatol 2015; 33:247-55. [PMID: 25704945].
3. Willmann G. Ultraviolet Keratitis: From the Pathophysiological Basis to Prevention and Clinical Management. High Alt Med Biol 2015; 16:277-82. [PMID: 26680683].
4. Muresan S, Filip A, Muresan A, Simon V, Moldovan R, Gal AF, Miclaus V. Histological findings in the Wistar rat cornea following UVB irradiation. Romanian journal of morphology and embryology = Rev Roum Morphol Embryol 2013; 54:247-52. .
5. Cejka C, Rosina J, Sirc J, Michalek J, Brunova B, Cejkova J. The reversibility of UV-B induced alterations in optical properties of the rabbit cornea depends on dose of UV irradiation. Photochem Photobiol 2013; 89:474-82. [PMID: 23106573].
6. Yin J, Huang Z, Wu B, Shi Y, Cao C, Lu Y. Lornoxicam protects mouse cornea from UVB-induced damage via inhibition of NF-{kappa}B activation. Br J Ophthalmol 2008; 92:562-8. [PMID: 18369073].
7. Chen BY, Lin DP, Wu CY, Teng MC, Sun CY, Tsai YT, Su KC, Wang SR, Chang HH. Dietary zerumbone prevents mouse cornea from UVB-induced photokeratitis through inhibition of NF-kappaB, iNOS, and TNF-alpha expression and reduction of MDA accumulation. Mol Vis 2011; 17:854-63. [PMID: 21527993].
8. Lin DP, Chang HH, Yang LC, Huang TP, Liu HJ, Chang LS, Lin CH, Chen BY. Assessment of ultraviolet B-blocking effects of weekly disposable contact lenses on corneal surface in a mouse model. Mol Vis 2013; 19:1158-68. [PMID: 23734085].
9. Chen BY, Lin DP, Chang LS, Huang TP, Liu HJ, Luk CP, Lo YL, Chang HH. Dietary alpha-lipoic acid prevents UVB-induced corneal and conjunctival degeneration through multiple effects. Invest Ophthalmol Vis Sci 2013; 54:6757-66. [PMID: 23989186].
10. Liou JC, Teng MC, Tsai YS, Lin EC, Chen BY. UV-blocking spectacle lens protects against UV-induced decline of visual performance. Mol Vis 2015; 21:846-56. [PMID: 26283865].
11. Ibrahim OM, Kojima T, Wakamatsu TH, Dogru M, Matsumoto Y, Ogawa Y, Ogawa J, Negishi K, Shimazaki J, Sakamoto Y, Sasaki H, Tsubota K. Corneal and retinal effects of

ultraviolet-B exposure in a soft contact lens mouse model. Invest Ophthalmol Vis Sci 2012; 53:2403-13. [PMID: 22410564].

12. Giblin FJ, Lin LR, Leverenz VR, Dang L. A class I (Senofilcon A) soft contact lens prevents UVB-induced ocular effects, including cataract, in the rabbit in vivo. Invest Ophthalmol Vis Sci 2011; 52:3667-75. [PMID: 21421866].
13. Chen SJ, Lee CJ, Lin TB, Liu HJ, Huang SY, Chen JZ, Tseng KW. Inhibition of Ultraviolet B-Induced Expression of the Proinflammatory Cytokines TNF-alpha and VEGF in the Cornea by Fucoxanthin Treatment in a Rat Model. Mar Drugs 2016; 14:13-[PMID: 26751458].
14. Agrawal RV, Murthy S, Sangwan V, Biswas J. Current approach in diagnosis and management of anterior uveitis. Indian J Ophthalmol 2010; 58:11-9. [PMID: 20029142].
15. Forrester JV, Klaska IP, Yu T, Kuffova L. Uveitis in mouse and man. Int Rev Immunol 2013; 32:76-96. [PMID: 23360160].
16. Pepple KL, Rotkis L, Van Grol J, Wilson L, Sandt A, Lam DL, Carlson E, Van Gelder RN. Primed Mycobacterial Uveitis (PMU): Histologic and Cytokine Characterization of a Model of Uveitis in Rats. Invest Ophthalmol Vis Sci 2015; 56:8438-48. [PMID: 26747775].
17. Xu Y, Chen W, Lu H, Hu X, Li S, Wang J, Zhao L. The expression of cytokines in the aqueous humor and serum during endotoxin-induced uveitis in C3H/HeN mice. Mol Vis 2010; 16:1689-95. [PMID: 20806043].
18. Qiu Y, Shil PK, Zhu P, Yang H, Verma A, Lei B, Li Q. Angiotensin-converting enzyme 2 (ACE2) activator diminazene aceturate ameliorates endotoxin-induced uveitis in mice. Invest Ophthalmol Vis Sci 2014; 55:3809-18. [PMID: 24854854].
19. Klaska IP, Forrester JV. Mouse models of autoimmune uveitis. Curr Pharm Des 2015; 21:2453-67. [PMID: 25777760].
20. Chang YH, Horng CT, Chen YH, Chen PL, Chen CL, Liang CM, Chien MW, Chen JT. Inhibitory effects of glucosamine on endotoxin-induced uveitis in Lewis rats. Invest Ophthalmol Vis Sci 2008; 49:5441-9. [PMID: 18719082].
21. Lennikov A, Kitaichi N, Noda K, Mizuuchi K, Ando R, Dong Z, Fukuhara J, Kinoshita S, Namba K, Ohno S, Ishida S. Amelioration of endotoxin-induced uveitis treated with the sea urchin pigment echinochrome in rats. Mol Vis 2014; 20:171-7. [PMID: 24520186].
22. Tuaillon N, Shen DF, Berger RB, Lu B, Rollins BJ, Chan CC. MCP-1 expression in endotoxin-induced uveitis. Invest Ophthalmol Vis Sci 2002; 43:1493-8. [PMID: 11980865].
23. Di Girolamo N, Verma MJ, McCluskey PJ, Lloyd A, Wakefield D. Increased matrix metalloproteinases in the aqueous humor of patients and experimental animals with uveitis. Curr Eye Res 1996; 15:1060-8. [PMID: 8921246].
24. Cuello C, Wakefield D, Di Girolamo N. Neutrophil accumulation correlates with type IV collagenase/gelatinase activity in endotoxin induced uveitis. Br J Ophthalmol 2002; 86:290-5. [PMID: 11864886].
25. Zigman S. Environmental near-UV radiation and cataracts. Optom Vis Sci 1995; 72:899-901. [PMID: 8749337].
26. Bansal S, Barathi VA, Iwata D, Agrawal R. Experimental autoimmune uveitis and other animal models of uveitis: An update. Indian J Ophthalmol 2015; 63:211-8. [PMID: 25971165].

Articles are provided courtesy of Emory University and the Zhongshan Ophthalmic Center, Sun Yat-sen University, P.R. China. The print version of this article was created on 12 April 2017. This reflects all typographical corrections and errata to the article through that date. Details of any changes may be found in the online version of the article.